Semiclassical Theory of Noise in Multielement Semiconductor Lasers

ROBERT J. LANG, STUDENT MEMBER, IEEE, AND AMNON YARIV, FELLOW, IEEE

Abstract—**We present a derivation of the noise spectra of multielement semiconductor lasers. We model the noise by a set of Langevin sources which drive a system of small-signal field equations. The Langevin sources are normalized to transition rates within the laser and general formulas for relative intensity, frequency fluctuation, and field spectra are produced. We evaluate the formulas for several specific cases of interest, including those of a passive–active resonator and active–active coupled cavity resonator. In each case, the linewidth is governed by effective α-parameter(s) which generally differ from the material parameter. In the active–active cavity, the linewidth consists of two parts, one which is similar to the Schawlow–Townes linewidth, and a second which is proportional to the FM modulation index.**

INTRODUCTION

SINGLE-mode semiconductor lasers are desirable for use as transmitters in fiber-optic systems because of their potential for high-speed modulation and narrow spectrum. The narrow spectrum minimizes dispersion as an optical pulse travels through a dispersive fiber, and consequently increases the available modulation bandwidth for a given length of fiber (or vice versa). Simple single-element Fabry–Perot lasers tend to oscillate in multiple longitudinal modes, however, particularly under current modulation. This property unnecessarily broadens the spectrum of the modulated signal. To restrict the laser to single-longitudinal mode operation, more complicated structures have been proposed, including distributed-feedback lasers [1], [2] and various geometries of coupled-cavity lasers [3]–[12].

Many of the laser geometries are plagued by chirping, or FM under current modulation [13], [14]. While this property may be desirable for an FM modulation system, it also broadens the spectrum of the modulated laser. Recently, it has been demonstrated that chirping in two-section lasers can be reduced by splitting the modulation current between the two sections [13] or by judicious selection of the bias point [12]. More recently, we derived analytic expressions for both the frequency and amplitude responses of a general multielement semiconductor laser [15] in terms of the bias point quantities. The knowledge of which physical quantities affect the chirp, resonance frequency, etc., allow one to design multielement lasers with a minimum of chirp under modulation.

The fundamental limit to the linewidth of the laser, however, is the noise associated with the process of spontaneous emission and quantization of the carriers and photons. In the past five years, the noise properties of semiconductor lasers have been the subject of scrutiny, and several anomalous features have been observed and explained, including a spiking resonance in the intensity spectrum [16], [17] and frequency fluctuation spectrum [18], a linewidth some 30 times greater than that predicted by the modified Schawlow–Townes theory [19], [20], power-independent linewidth components [21], asymmetry in the field spectrum [18], and excess noise at low frequencies in both the intensity and frequency fluctuation spectrum [22]–[24], [28].

To our knowledge, there have been no attempts to date at analyzing the noise properties of semiconductor lasers with multiple active elements. Recently, it was observed [25], [26] that phase noise could be reduced in a passive–active laser by varying the coupling between the cavities, and it seems likely that such would be the case in an active–active cavity. On the other hand, coupled-cavity lasers are known to possess an FM response to current fluctuations, which may increase the fundamental linewidth even in the absence of modulation. A theory of multielement laser noise would be useful in evaluating multielement lasers for systems applications.

A common technique for analyzing noise properties is to model the noise by a Langevin (white) source with an appropriate normalization which drives the rate equations of the system in question [27]–[30]. In this paper, we apply the Langevin theory to small-signal rate equations to calculate the spectra of a multielement laser. In Section II, we develop the small-signal linear rate equations from the nonlinear equations describing the dynamics of the laser and introduce the Langevin driving sources. In Section III, we normalize the Langevin sources and calculate their correlations and spectra. In Section IV, we combine the results of Sections II and III to produce general formulas for the relative intensity spectra, frequency fluctuation spectra, and field spectra of an arbitrary multielement semiconductor laser. In addition, we evaluate some of the formulas for several specific cases. In Section V, we summarize the important results of the analysis.

Manuscript received July 18, 1985; revised October 18, 1985. This work was supported by grants from the Office of Naval Research, ITT Corporation, Rockwell International, and the Air Force Office of Scientific Research. The work of R. J. Lang was supported by a fellowship from the National Science Foundation.

The authors are with the California Institute of Technology, Pasadena, CA 91125.

IEEE Log Number 8407060.

0018-9197/86/0300-0436$01.00 © 1986 IEEE

II. Rate Equations

The system we are considering in a semiconductor laser consisting of N active elements (and an arbitrary number of passive elements). For each active element, the carrier dynamics can be described by volume-averaged rate equations as

$$\dot{n}_i = \frac{J_i}{qd} - \frac{n_i}{\tau_s} - g_i(n_i)\, p_i \tag{1}$$

where n_i is the carrier density in the ith cavity, J_i is the pump current density, q is the charge on an electron, d is the active layer thickness, τ_s is the spontaneous lifetime, $g_i(n_i)$ is the gain constant (as a function of the carrier density), and p_i is the photon density in the ith cavity.

The DC operation of the resonator (threshold carrier density and lasing frequency) is governed by a dispersion relation of the form

$$F(\omega, n_1, \cdots n_N) = 0 \tag{2}$$

particular to the geometry under consideration. The derivation of (2) has been carried out for several geometries of interest [5]–[12], and is generally straightforward. In Section IV we will derive the dispersion function F for those systems which we consider in detail, but for now we will assume that it exists and is known. We will also require a set of fill factors defined by

$$\Gamma_i(\omega, n_1, \cdots n_N) \equiv \frac{p_i}{p} \tag{3}$$

where p is the average photon density in the composite cavity, and ω in (3) is implicitly defined by (2) as a complex function of the carrier densities $\{n_i\}$.

In an earlier work, we showed that if one takes the electric field amplitude to be of the form $e^{i\psi(t)}$, then the dispersion equation (2) is an instantaneously valid description of the dynamics of the system if we replace ω by $\dot{\psi}$. The result is a first-order nonlinear differential equation for the field amplitude and phase [15]. We substitute (3) in (1) and linearize (1) and (2) about a steady-state operating point

$$\begin{aligned} J_i &\equiv J_{i0} + qd \cdot e_i(t) \\ n_i &\equiv n_{i0} + \nu_i(t) \\ \dot{\psi} &\equiv \omega_0 + \Delta\omega(t) - j\dot{\rho}(t) \end{aligned} \tag{4}$$

which yields

$$\dot{\rho} = \sum_i g'_{i\text{eff}} \nu_i \tag{5}$$

$$\Delta\omega = -\sum_i m'_{i\text{eff}} \nu_i \tag{6}$$

$$\dot{\nu}_i = e_i - \left[\frac{1}{\tau_s} + g'_i \Gamma_i p\right] \nu_i - 2 g_i \Gamma_i p \rho - \sum_k g_i p \frac{d\Gamma_i}{dn_k} \nu_k \tag{7}$$

where

$$g'_{i\text{eff}} \equiv \text{Im}\, \frac{\partial F/\partial n_i}{\partial F/\partial \omega}, \qquad m'_{i\text{eff}} \equiv \text{Re}\, \frac{\partial F/\partial n_i}{\partial F/\partial \omega} \tag{8}$$

$$\frac{d\Gamma_i}{dn_k} = \frac{\partial \Gamma_i}{\partial n_k} - m'_{k\text{eff}} \frac{\partial \Gamma_i}{\partial\, \text{Re}\,(\omega)} - g'_{k\text{eff}} \frac{\partial \Gamma_i}{\partial\, \text{Im}\,(\omega)} \tag{9}$$

and all derivatives are evaluated at the operating point. Equations (5)–(7) are now a set of linear differential equations giving the response to a small modulation.

We Fourier transform (5)–(7) (so that the operator d/dt becomes a factor $j\Omega$), and we denote transformed dynamical variables by a tilde. We make the following definitions:

$$\begin{aligned} &\frac{1}{\tau_i} \equiv \frac{1}{\tau_s} + g'_i \Gamma_i p, \quad \omega^2_{i\text{eff}} \equiv 2 g'_{i\text{eff}} g_i \Gamma_i p, \\ &\alpha_{i\,\text{eff}} \equiv m'_{i\text{eff}} / g'_{i\text{eff}} \\ &d_i \equiv j\Omega + \frac{1}{\tau_i}, \quad c_{ik} \equiv p g_i \frac{d\Gamma_i}{dn_k}. \end{aligned} \tag{10}$$

The transformed equations, now linear algebraic, can be put into matrix form as

$$\begin{pmatrix} j\Omega & 0 & -g'_{1\text{eff}} & \cdots & -g'_{N\text{eff}} \\ 0 & 1 & \alpha_{1\text{eff}} g'_{1\text{eff}} & \cdots & \alpha_{N\text{eff}} g'_{N\text{eff}} \\ \dfrac{\omega^2_{1\text{eff}}}{g'_{1\text{eff}}} & 0 & c_{11} + d_1 & \cdots & c_{N1} \\ \vdots & \vdots & \vdots & & \vdots \\ \dfrac{\omega^2_{N\text{eff}}}{g'_{N\text{eff}}} & 0 & c_{N1} & \cdots & c_{NN} + d_N \end{pmatrix} \cdot \begin{pmatrix} \tilde{\rho} \\ \Delta\tilde{\omega} \\ \tilde{\nu}_1 \\ \vdots \\ \tilde{\nu}_N \end{pmatrix} = \begin{pmatrix} 0 \\ 0 \\ \tilde{e}_1 \\ \vdots \\ \tilde{e}_N \end{pmatrix}. \tag{11}$$

Equation (11) defines the small-signal response of the field amplitude ($\tilde{\rho}$), frequency ($\Delta\tilde{\omega}$), and carrier densities ($\tilde{\nu}_i$) to fluctuations in the pump current ($\tilde{e}_i$). Had we some physical mechanism for directly driving the amplitude or phase, that, too, could be incorporated into the right side of (11). In the next section, we develop the appropriate Langevin sources for insertion into (11).

III. Langevin Sources

When several systems of particles interact with each other and/or with external baths through random particle interactions, there are fluctuations associated with each interaction. Such fluctuations can be accounted for by including appropriately normalized Langevin sources into the equations of motion. This approach can also be used with variables which vary continuously (e.g., temperature, phase [27]) but the normalization procedure is not as clear-cut as it is for particulate variables. In the latter case, each independent number variable $\{A\}$ will have associated with it a fluctuation source $\{a\}$ which satisfies

$$\langle a(t)\, a(t')\rangle = \left\langle \frac{dA}{dt} \right\rangle \delta(t-t') \qquad (12)$$

where $\langle\ \rangle$ denotes ensemble average. The source $\{a\}$ is then used to drive the rate equation for the fluctuations in $\{A\}$. If there is more than one independent mechanism creating particle fluxes into or out of the number variable pool, there will be a driving source associated with each transition rate. Alternatively, the various sources may be lumped into a single source whose autocorrelation is the sum of the individual sources (as is done here).

In our system, the number variables are total photon number in the optical mode, and carrier number in each cavity. Thus, for the photon number, the appropriate Langevin source possesses the autocorrelation

$$\langle s(t)\, s(t')\rangle \equiv \left[\sum_i (R_i^{STE} + R_i^{STA} + \beta R_i^{SPE}) + R^{CAV}\right] \cdot \delta(t-t') \qquad (13)$$

where R_i^{STE} is the stimulated emission rate from cavity i, R_i^{STA} is the stimulated absorption rate, R_i^{SPE} is the spontaneous emission rate, R_i^{CAV} is the cavity loss rate, and β is the fraction of spontaneous emission rate coupled into the optical mode. For carrier number in cavity i, we have

$$\langle c_i(t)\, c_i(t')\rangle \equiv [R_i^{STE} + R_i^{STA} + R_i^{SPE} + R_i^{PMP}]\, \delta(t-t') \qquad (14)$$

where R_i^{PMP} is the pump rate into cavity i.

Since $\beta \approx 10^{-4}$, we can drop it from (13); in addition, balancing input and output flows from the particle pools yields the relations

$$R^{CAV} = \sum_i R_i^{STE} - R_i^{STA}, \quad R_i^{PMP} = R_i^{STE} - R_i^{STA}. \qquad (15)$$

Also, if we introduce the spontaneous emission factors

$$\eta_i = \frac{R_i^{STE}}{R_i^{STE} - R_i^{STA}} \qquad (16)$$

we can relate these rates to the variables in the rate equations

$$R_i^{STE} - R_i^{STA} = V_i g_i \Gamma_i p, \quad R_i^{STE} = n_i/\tau_s. \qquad (17)$$

The Langevin sources possess nonzero cross correlations whenever an event changes two variables at once (which stimulated emission and absorption do; spontaneous emission does also but the cross-correlation is on the order of β and can safely be ignored). The cross-correlations of interest are

$$\langle s(t)\, c_i(t')\rangle = -(R_i^{STE} + R_i^{STA})\, \delta(t-t')$$
$$\langle c_i(t)\, c_i(t')\rangle = 0 \qquad \text{for } i \neq j. \qquad (18)$$

We should now convert these Langevin sources appropriate for number variables to sources appropriate for the variables in our system—namely, relative amplitude and carrier density. If we define the sources as Δ for relative amplitude and Ξ_i for carrier density, then

$$s = 2pV\Delta, \quad c_i = V_i \Xi_i \qquad (19)$$

where V is the total volume of the optical mode and V_i is the volume of the ith active element. The phase, too, is subject to random fluctuations due to spontaneous emission. Being a continuous variable, the correlations of its Langevin source Φ are not as immediately obvious as those of the amplitude and carrier sources. Using a model discussed by Henry [20], Vahala *et al.* have shown [26] that the Langevin source driving the phase has the same autocorrelation as that of the source driving the amplitude fluctuations but is uncorrelated with any other source. (Although they were considering only a single-element laser, their argument is independent of the number of separate active regions.) Using (15)–(17) to put the transition rates in terms of the rate equation variables, we can summarize the relevant correlations for the amplitude Langevin source Δ, the phase source Φ, and the carrier sources Ξ as

$$\langle \Delta(t)\, \Delta(t')\rangle = \langle \Phi(t)\, \Phi(t')\rangle = \frac{1}{2pV^2} \sum_i \eta_i g_i \Gamma_i V_i \delta(t-t') \qquad (20)$$

$$\langle \Xi_i(t)\, \Xi_j(t')\rangle = \frac{2}{V_i}\left[\frac{n_i}{\tau_s} + \eta_i g_i \Gamma_i p\right] \delta_{ij}\delta(t-t') \qquad (21)$$

$$\langle \Delta(t)\, \Xi_i(t')\rangle = -\frac{g_i\Gamma_i}{2V}(2\eta_i - 1)\, \delta(t-t'). \qquad (22)$$

All other cross-correlations are zero. Equation (11) is in terms of transformed variables, so it is convenient to cast (19)–(22) in the same manner, particularly since we are interested in spectral functions $W_{fg}(\Omega)$ which are themselves transformed quantities. Mathematical problems arise when one attempts to transform a stationary signal, however; to be rigorous, one must use finite-domain Fourier transforms defined as follows:

$$\tilde{f}_T(\omega) \equiv \int_{-T/2}^{+T/2} dt\, f(t)\, e^{-j\omega t},$$
$$\tilde{g}_T(\omega) \equiv \int_{-T/2}^{+T/2} dt\, g(t)\, e^{-j\omega t}. \qquad (23)$$

Then one can calculate the spectral quantities defined by the Wiener–Khintchine relations as

$$W_{fg}(\Omega) \equiv \int d\tau \langle f(at)\, g(t+\tau)\rangle\, e^{-j\Omega\tau} \qquad (24)$$

from the finite-domain transforms by

$$W_{fg}(\Omega) = \lim_{T\to\infty} \frac{\langle \tilde{f}_T(\Omega)\, \tilde{g}_T(-\Omega)\rangle}{T}. \qquad (25)$$

Strictly speaking, the relations that make the Fourier transform useful (transformation of differential operators) do not hold as long as the object of the transform is finite at the limits of integration; for example, the derivative transforms as

$$\int_{-T/2}^{+T/2} dt\, \frac{df}{dt}\, e^{-j\omega t} = f(t)\, e^{-j\omega t}\Big|_{-T/2}^{T/2} + j\omega \tilde{f}_T(\omega). \tag{26}$$

However, the first term on the right in (26) (and others like it) drop out after ensemble averaging and dividing by T in (25). Therefore, we will continue to use properties of infinite-domain transforms with the understanding that at some point down the line, we will perform the average and limit of (25). Questions of validity and existence aside, we can calculate the spectra of the Langevin sources in (19)–(22) directly from (24). They are

$$W_{\Delta\Delta}(\Omega) = W_{\Phi\Phi}(\Omega) = \frac{1}{2pV^2} \sum_i \eta_i g_i \Gamma_i V_i \tag{27}$$

$$W_{\Xi_i \Xi_j}(\Omega) = \frac{2}{V_i}\left[\frac{n_i}{\tau_s} + \eta_i g_i \Gamma_i p\right] \delta_{ij} \tag{28}$$

$$W_{\Xi_i \Delta}(\Omega) = W_{\Delta \Xi_i}(\Omega) = -\frac{g_i \Gamma_i}{2V}(2\eta_i - 1). \tag{29}$$

All spectra of Langevin sources are white; all other spectra between sources are zero.

IV. Fluctuation Spectra

A. General Formulas

At this point, we insert our appropriately normalized Langevin sources into the driving term of the small-signal equations, that is, the right side of (11). In the absence of external modulation ($\tilde{e}_i \equiv 0$), the result is

$$\begin{pmatrix} j\Omega & -g'_{1\text{eff}} & \cdots & -g'_{N\text{eff}} \\ 0 & \alpha_{1\text{eff}} g'_{1\text{eff}} & \cdots & \alpha_{N\text{eff}} g'_{N\text{eff}} \\ \dfrac{\omega^2_{1\text{eff}}}{g'_{1\text{eff}}} & c_{11} + d_1 & \cdots & c_{1N} \\ \vdots & \vdots & & \vdots \\ \dfrac{\omega^2_{N\text{eff}}}{g'_{N\text{eff}}} & c_{N1} & \cdots & c_{NN} + d_N \end{pmatrix} \cdot \begin{pmatrix} \tilde{\rho} \\ \Delta\tilde{\omega} \\ \tilde{\nu}_1 \\ \vdots \\ \tilde{\nu}_N \end{pmatrix} = \begin{pmatrix} \tilde{\Delta} \\ \tilde{\Phi} \\ \tilde{\Xi} \\ \vdots \\ \tilde{\Xi}_N \end{pmatrix} \tag{30}$$

recognizing, as we said, that the transforms exist only for finite intervals. Now the formulation is complete; by inverting (30), we can write each response $\{\tilde{\rho}, \Delta\tilde{\omega}, \tilde{\nu}_i\}$ as a linear combination of the Langevin sources $\{\tilde{\Delta}, \tilde{\Phi}, \tilde{\Xi}_i\}$, and consequently write spectral functions of the response elements [e.g., $W_{\rho\rho}(\Omega)$] as linear combinations of the previously defined spectra of the Langevin sources (e.g., $W_{\Delta\Delta}$).

Equation (30) can be solved using Cramer's rule, yielding

$$\tilde{\rho}(\Omega) = \frac{\begin{vmatrix} \tilde{\Delta} & -g'_{1\text{eff}} & \cdots & -g'_{N\text{eff}} \\ \tilde{\Xi}_1 & c_{11} + d_1 & \cdots & c_{1N} \\ \vdots & \vdots & & \vdots \\ \tilde{\Xi}_N & c_{N1} & \cdots & c_{NN} + d_N \end{vmatrix}}{\begin{vmatrix} j\Omega & -g'_{1\text{eff}} & \cdots & -g'_{N\text{eff}} \\ \dfrac{\omega^2_{1\text{eff}}}{g'_{1\text{eff}}} & c_{11} + d_1 & \cdots & c_{1N} \\ \vdots & \vdots & & \vdots \\ \dfrac{\omega^2_{N\text{eff}}}{g'_{N\text{eff}}} & c_{N1} & \cdots & c_{NN} + d_N \end{vmatrix}} \tag{31}$$

$$\Delta\tilde{\omega} = \frac{\begin{vmatrix} j\Omega & \tilde{\Delta} & -g'_{1\text{eff}} & \cdots & -g'_{N\text{eff}} \\ 0 & \tilde{\Phi} & \alpha_{1\text{eff}} g'_{1\text{eff}} & \cdots & \alpha_{N\text{eff}} g'_{N\text{eff}} \\ \dfrac{\omega^2_{1\text{eff}}}{g'_{1\text{eff}}} & \tilde{\Xi}_1 & c_{11} + d_1 & \cdots & c_{1N} \\ \vdots & \vdots & \vdots & & \vdots \\ \dfrac{\omega^2_{N\text{eff}}}{g'_{N\text{eff}}} & \tilde{\Xi}_N & c_{N1} & \cdots & c_{NN} + d_N \end{vmatrix}}{\begin{vmatrix} j\Omega & -g'_{1\text{eff}} & \cdots & -g'_{N\text{eff}} \\ \dfrac{\omega^2_{1\text{eff}}}{g'_{1\text{eff}}} & c_{11} + d_1 & \cdots & c_{1N} \\ \vdots & \vdots & & \vdots \\ \dfrac{\omega^2_{N\text{eff}}}{g'_{N\text{eff}}} & c_{N1} & \cdots & c_{NN} + d_N \end{vmatrix}} \tag{32}$$

$$\tilde{\nu}_i = \frac{\begin{vmatrix} j\Omega & -g'_{1\text{eff}} & \cdots & -g'_{(i-1)\text{eff}} & \tilde{\Delta} & \cdots & -g'_{N\text{eff}} \\ \dfrac{\omega_{1\text{eff}}^2}{g'_{1\text{eff}}} & c_{11}+d_1 & \cdots & c_{1(i-1)} & \tilde{\Xi}_1 & \cdots & c_{1N} \\ \vdots & \vdots & & \vdots & \vdots & & \vdots \\ \dfrac{\omega_{N\text{eff}}^2}{g'_{N\text{eff}}} & d_{N1} & \cdots & c_{(i-1)} & \tilde{\Xi}_N & \cdots & c_{NN}+d_N \end{vmatrix}}{\begin{vmatrix} j\Omega & -g'_{1\text{eff}} & \cdots & -g'_{N\text{eff}} \\ \dfrac{\omega_{1\text{eff}}^2}{g'_{1\text{eff}}} & c_{11}+d_1 & \cdots & c_{1N} \\ \vdots & \vdots & & \vdots \\ \dfrac{\omega_{N\text{eff}}^2}{g'_{N\text{eff}}} & c_{N1} & \cdots & c_{NN}+d_N \end{vmatrix}} \tag{33}$$

So, a spectral term $W_{fg}(\Omega)$ is given by

$$W_{fg}(\Omega) = \lim_{T\to\infty} \frac{\langle \tilde{f}(\Omega)\, \tilde{g}(-\Omega)\rangle}{T} \tag{34}$$

and we can produce this by multiplying the expressions for $\tilde{f}(\Omega)$ and $\tilde{g}(-\Omega)$ together and replacing each product of Langevin sources (e.g., $\tilde{\Delta}\tilde{\Delta}$) by the associated spectral quantity (e.g., $W_{\Delta\Delta}$). In this manner one can produce any desired spectral quantity. We shall not carry this process out in full generality (although the prescription is here for anyone so inclined). Instead, we shall spend the rest of the paper deriving spectra for some specific devices of interest.

B. Single-Element Fabry–Perot Laser

To begin to get a feel for how to use (27)–(29) and (31)–(33) to calculate spectra, let us first rederive the noise spectra for a single-element, simple two-mirror resonator. As pointed out previously, the term c_{11} can be absorbed into $1/\tau_1$, so that when we evaluate (31) and (32) we get

$$\tilde{\rho}(\Omega) = \frac{(j\Omega + 1/\tau_1)\,\tilde{\Delta} + g'_{1\text{eff}}\tilde{\Xi}_1}{\omega_{1\text{eff}}^2 - \Omega^2 + j\Omega/\tau_1} \tag{35}$$

$$\Delta\tilde{\omega}(\Omega) = \tilde{\Phi} + \alpha_{1\text{eff}} \frac{\omega_{1\text{eff}}^2\tilde{\Delta} - j\Omega g'_{1\text{eff}}\tilde{\Xi}_1}{\omega_{1\text{eff}}^2 - \Omega^2 + j\Omega/\tau_1} \tag{36}$$

which leads to the relative intensity spectrum

$$W_{\rho\rho}(\Omega) = \frac{(\Omega^2 + 1/\tau_1^2)\, W_{\Delta\Delta} + 2g'_{1\text{eff}}W_{\Delta\Xi_1}/\tau_1 + g'^2_{1\text{eff}}W_{\Xi_1\Xi_1}}{(\omega_{1\text{eff}}^2 - \Omega^2)^2 + \Omega^2/\tau_1^2} \tag{37}$$

and the frequency fluctuation spectrum

$$W_{\omega\omega}(\Omega) = W_{\Phi\Phi} + \alpha_{1\text{eff}}^2 \frac{\omega_{1\text{eff}}^4 W_{\Delta\Delta} + \Omega^2 g'^2_{1\text{eff}} W_{\Xi_1\Xi_1}}{(\omega_{1\text{eff}}^2 - \Omega^2)^2 + \Omega^2/\tau_1^2}. \tag{38}$$

Now we substitute in the normalizations for the Langevin sources

$$W_{\rho\rho}(\Omega) = \frac{1}{2pV}\left\{\left[(\Omega^2 + 1/\tau_1^2)\left(\eta_1 g_1 \Gamma_1 \frac{V_1}{V}\right) + 4g'_{1\text{eff}}p\,\frac{V}{V_1} \cdot \left(\frac{n_1}{\tau_s} + \eta_1 g_1\Gamma_1 p\right) - (2\eta_1 - 1)\,\omega_{1\text{eff}}^2/\tau_1 \Big/ (\omega_{1\text{eff}}^2 - \Omega^2)^2 + \Omega^2/\tau_1^2 \right]\right\} \tag{39}$$

$$W_{\omega\omega}(\Omega) = \frac{\eta_1 g_1 \Gamma_1}{2pV}\left[1 + \alpha_{1\text{eff}}^2 \frac{\omega_{1\text{eff}}^4}{(\omega_{1\text{eff}}^2 - \Omega^2)^2 + \Omega^2/\tau_1^2}\right] + \frac{2}{V}\,\frac{\alpha_{1\text{eff}}^2\Omega^2 g'^2_{1\text{eff}}\left(\dfrac{n_1}{\tau_s} + \eta_1 g_1 \Gamma_1 p\right)}{(\omega_{1\text{eff}}^2 - \Omega^2)^2 + \Omega^2/\tau_1^2}. \tag{40}$$

We recognize the above as the relative intensity and frequency fluctuation spectrum of a simple single-cavity, two-mirror laser [26]. Of particular interest is the contribution of the frequency fluctuation spectrum to the linewidth. If amplitude fluctuations are negligible or suppressed in measurement, then the field spectrum $W_\epsilon(\omega_0 + \omega)$ (where ω is the deviation from the lasing frequency ω_0) is [27]

$$W_\epsilon(\omega + \omega_0) = \frac{1}{2}E_0^2 \,\mathrm{Re}\int_{-\infty}^{+\infty} d\tau\, e^{-j\omega\tau} \cdot \exp\left[\frac{-\tau^2}{2\pi}\int_0^\infty d\Omega\, W_{\omega\omega}(\Omega)\left(\frac{\sin \Omega\tau/2}{\Omega\tau/2}\right)^2\right] \tag{41}$$

in which E_0 is the field amplitude. If $W_{\omega\omega}$ is a sum of several components, then the field spectrum is the convolution of the spectrum computed individually from each of the components. While high-frequency structure in the spectrum of $W_{\omega\omega}$ is responsible for structure in the field spectrum (e.g., sidebands at the relaxation resonance [26]), the dominant contribution to linewidth comes from the $\Omega = 0$ component of $W_{\omega\omega}$. It in fact produces a Lorentzian with linewidth exactly equal to $W_{\omega\omega}(0)$ [27]. Examination of (40) shows that the linewidth of a single-element laser is

$$W_{\omega\omega}(0) = \frac{\eta_1 g_1 \Gamma_1}{2pV}(1 + \alpha_{1\text{eff}}^2) \tag{42}$$

that is, the enhanced modified Schawlow–Townes linewidth [20]. To calculate $\alpha_{1\text{eff}}$, we recall that the dispersion equation for a single-element, two-mirror laser is

$$F(\omega, n_1) \equiv \frac{1}{R^2}\exp\left[(\gamma_1(n_1) - \gamma_0)\, L_1 - \frac{2j\omega\mu_1(n_1)\, L_1}{c}\right] - 1 = 0 \tag{43}$$

where $\gamma_1(n_1)$ is the power gain per unit length, γ_0 is the loss, L_1 is the length of the laser, $\mu_1(n_1)$ is the index of refraction, and R is the mirror reflectivity. Applying relations (8) and (10) to (43), we get

$$g'_{1\,\text{eff}} = \frac{\gamma'_1 c}{2\mu_1}, \quad m'_{1\,\text{eff}} = \frac{\omega\mu'_1}{\mu_1}, \quad \alpha_{1\,\text{eff}} = \frac{2\omega\mu'_1}{\gamma'_1 c} \tag{44}$$

where a prime on a material parameter denotes differentiation with respect to the carrier density. So, for this configuration, the effective modulation quantities are equal to the material modulation quantities, which is, in fact, what we expect from the conventional theory.

C. Passive–Active Coupled Cavity

The above situation (effective parameters = material parameters) does not always hold, even for single-active-element cavities. The addition of a passive element to the resonator (e.g., an external cavity) changes the dispersion equation, and consequently alters the effective modulation parameters; their values end up depending upon the relative tuning of the two cavities. We shall now treat the case of an active element coupled to a passive cavity, illustrated in Fig. 1. Two cavities of length L_1 and L_2 are coupled via an effective mirror (e.g., an air gap; the length of the gap may be zero as long as the discontinuity remains) with transmission and reflection coefficients T_2 and R_2, respectively. (In all calculations and graphs which follow, we will assume the following material parameters: loss $\gamma_0 = 80$ cm^{-1}, nonresonant refractive index $\mu_{\text{GaAs}} = 3.5$, and linewidth enhancement factor $\alpha_{\text{GaAs}} = -5$.) The resonance condition is determined by requiring that the field reproduce itself after one roundtrip through the composite structure. Following the approach of Henry [20], we find that the field E'_1 at the coupler results from reflection of E_1 and transmission of E_2:

$$E'_1 = R_2 E_1 + T_2 E_1 \tag{45}$$

while the roundtrip through cavity 1 results in

$$E_1 = R_1 \exp\left[(\gamma_1 - \gamma_0) L_1 - 2j\omega\mu_1 L_1/c\right] E'_1. \tag{46}$$

A similar pair of equations holds for E'_2 and E_2. To minimize the algebra, let us define

$$\begin{aligned} \varphi_1(\omega, n_1) &\equiv -(\gamma_1 - \gamma_0) L_1 + 2j\omega\mu_1 L_1/c - \ln R_1 R_2, \\ \varphi_2(\omega) &\equiv 2j\omega\mu_2 L_2/c - \ln R_3 R_2 \\ K^{1/2} &\equiv \frac{T_2}{R_2}. \end{aligned} \tag{47}$$

Then (45) and (46) and their companion equations for cavity (2) yield

$$[e^{\varphi_1} - 1]\, E_1 = K^{1/2} E_2, \quad [e^{\varphi_2} - 1]\, E_2 = K^{1/2} E_1. \tag{48}$$

Eliminating the field variables yields the dispersion equation

$$F(\omega, n_1) \equiv [e^{\varphi_1} - 1][e^{\varphi_2} - 1] - K = 0. \tag{49}$$

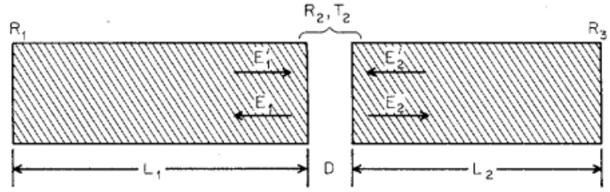

Fig. 1. Schematic of a longitudinally-coupled-cavity laser. Cavity 2 may be either passive or active. E'_1 and E'_2 are the fields incident upon a gap of width D. L_1 and L_2 are the lengths of cavities 1 and 2, respectively.

If the gain per unit length is not too large, then it is a good approximation to take the photon density in the ith cavity as proportional to $|E_i|^2$. (More exact results can be obtained by integrating the fields in each cavity, but in the interest of obtaining maximum information for minimum algebra, we shall use the approximate results.) Manipulation of (48) gives the fill factor

$$\Gamma_1 = \frac{|e^{\varphi_1} - 1|\,(L_1 + L_2)}{|e^{\varphi_1} - 1|\, L_2 + |e^{\varphi_2} - 1|\, L_1}. \tag{50}$$

The effective modulation quantities $g'_{1\,\text{eff}}$, $m'_{1\,\text{eff}}$ are determined by (18) in terms of partial derivatives of (49), evaluated at the operating point. Unfortunately, (49) is a transcendental equation that must be solved numerically. We can find approximate solutions for weak coupling between the cavities, however (that is, $K \ll 1$) by doing a perturbation series in K.

For small coupling, we can treat the passive resonator as providing a frequency-dependent load on the other; we expand ω in a perturbation series

$$\omega \equiv \omega_0 + \omega_1 + O(K^2) \tag{51}$$

where ω_1 is $O(K)$. The zeroth order equation is

$$[e^{\varphi_1(\omega_0)} - 1][e^{\varphi_2(\omega_0)} - 1] = 0. \tag{52}$$

If cavity 2 possesses no gain, then the right bracket of (52) cannot be zero near threshold. Thus, we take the left bracket equal to zero.

$$[e^{\varphi_1(\omega_0)} - 1] = 0 \rightarrow \omega_0 = \frac{c}{\mu_1 L_1}\left\{k\pi + \frac{1}{2j}\left[(\gamma_1 - \gamma_0) L_1 + \ln R_1 R_2\right]\right\} \tag{53}$$

where k is an arbitrary integer, chosen such that ω_0 is close to the peak of the gain spectrum. The next order of the perturbation sequence is

$$\omega_1 = K \frac{c}{\mu_1 L_1} [e^{\varphi_2(\omega_0)} - 1]^{-1} \tag{54}$$

ω_1 represents the effect of the detuned loading upon the resonance ω_0. The imaginary part of ω_1 changes the threshold gain which provides gain selectivity between modes, while the real part pulls the resonance frequency.

Explicitly evaluating $\varphi_2(\omega_0)$, we find

$$\varphi_2(\omega_0) = \frac{\mu_2 L_2}{\mu_1 L_1} 2jk\pi + \frac{\mu_2 L_2}{\mu_1 L_1} (\gamma_1 - \gamma_0) L_1 + \frac{\mu_2 L_2}{\mu_1 L_1} \ln R_1 R_2 - \ln R_2 R_3. \tag{55}$$

We use the expression for ω_0 and ω_1 with (51) to formulate a new, approximate dispersion equation

$$F(\omega, n_1) \equiv \omega - \frac{c}{\mu_1 L_1} \left\{ k\pi + \frac{(\gamma_1 - \gamma_0) L_1 + \ln R_1 R_2}{2j} + \frac{K}{2j} [e^{\varphi_2(\omega_0)} - 1]^{-1} \right\} = 0. \tag{56}$$

Now we can use this approximate equation to find the steady-state lasing frequency $\overline{\omega}$ and threshold gain $\gamma_1(n_{1\text{th}})$, and subsequently the effective modulation parameters $g'_{1\text{eff}}$, $m'_{1\text{eff}}$, and $\alpha_{1\text{eff}}$ to order K.

$$\overline{\omega} = \frac{c}{\mu_1 L_1} \left\{ k\pi + \frac{1}{2} \operatorname{Im} \frac{K}{[e^{\varphi_2(\omega_0)} - 1]} \right\}.$$

$$\gamma_1(n_{1\text{th}}) = \left[\gamma_0 - \frac{1}{L_1} \ln R_1 R_2 \right] - \frac{1}{L_1} \operatorname{Re} \frac{K}{[e^{\varphi_2(\omega_0)} - 1]}. \tag{58}$$

(Since μ_1 depends upon $n_{1\text{th}}$, the way to evaluate (57) and (58) is to use the zeroth-order part of (58) to calculate $n_{1\text{th}}$, and then use this value to find $\mu_1(n_{1\text{th}})$ for use in the first-order equations for $\overline{\omega}$ and γ_1.) In a passive–active resonator, the most conveniently tunable parameter is the length of the passive cavity L_2, so we have plotted the threshold gain and lasing frequency, respectively, for $K = -0.4$ in Figs. 2 and 3 and for $K = +0.4$ in Figs. 10 and 11.

The effective modulation parameters are given by (8) to be

$$\begin{Bmatrix} g'_{1\text{eff}} \\ m'_{1\text{eff}} \end{Bmatrix} = \begin{Bmatrix} \text{Im} \\ \text{Re} \end{Bmatrix} \left(\frac{\overline{\omega}\mu'_1}{\mu_1} - \frac{1}{2j} \frac{\gamma'_1 c}{\mu_1} \right) \cdot \left(1 + K \frac{\mu_2 L_2}{\mu_1 L_1} \frac{e^{\varphi_2(\omega_0)}}{[e^{\varphi_2(\omega_0)} - 1]^2} \right). \tag{59}$$

Recall that the material parameters g'_1 and m'_1 were given by

$$g'_1 \equiv \frac{\gamma'_1 c}{2\mu_1}, \quad m'_1 \equiv \frac{\overline{\omega}\mu'_1}{\mu_1} \tag{60}$$

and define the complex quantity

$$\nu \equiv K \frac{\mu_2 L_2}{\mu_1 L_1} \frac{e^{\varphi_2(\omega_0)}}{[e^{\varphi_2(\omega_0)} - 1]^2}. \tag{61}$$

Then, denoting real and imaginary parts of ν by an r and i subscript, respectively, the effective modulation parameters are given by

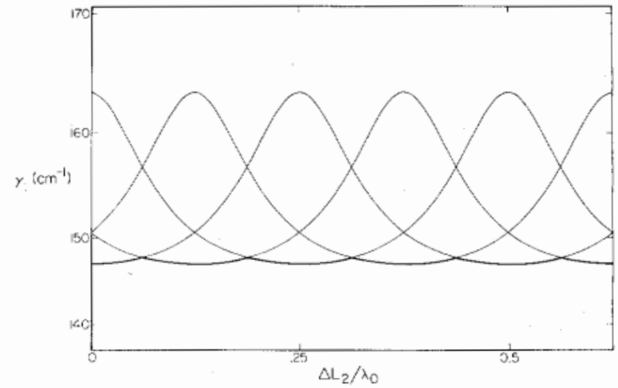

Fig. 2. Threshold gain for several modes as a function of passive cavity length in a (200–175 μm) active–passive laser, with a coupling factor $K = -0.4$. Heavy lines indicate the lasing mode, i.e., the mode with the lowest threshold gain.

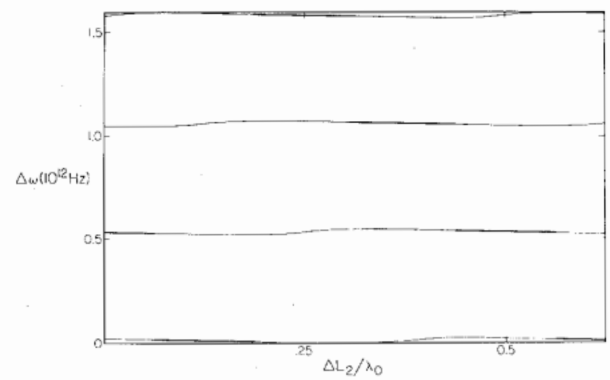

Fig. 3. Lasing frequency versus cavity length for the device of Fig. 2, showing the effects of frequency pulling on each mode. As in Fig. 2, the heavy line indicates the lasing mode.

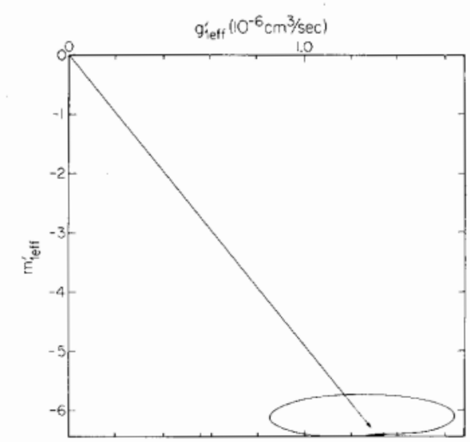

Fig. 4. Trajectory of $g'_{1\text{eff}}$, $m'_{1\text{eff}}$ in the g', m' plane for the device of Fig. 2. The slope of a vector from the origin to a point on the tuning curve gives the effective α-parameter. The vector connecting the origin to the point in the interior of the trajectory corresponds to the material quantities g', m'.

$$g'_{1\text{eff}} = g'_1(1 + \nu_r) + \nu_i m'_1,$$
$$m'_{1\text{eff}} = m'_1(1 + \nu_r) - \nu_i g'_1. \tag{62}$$

From (62) we see that the effect of the passive cavity is to "mix" the material differential gain and index to produce the effective quantities. For negative imaginary val-

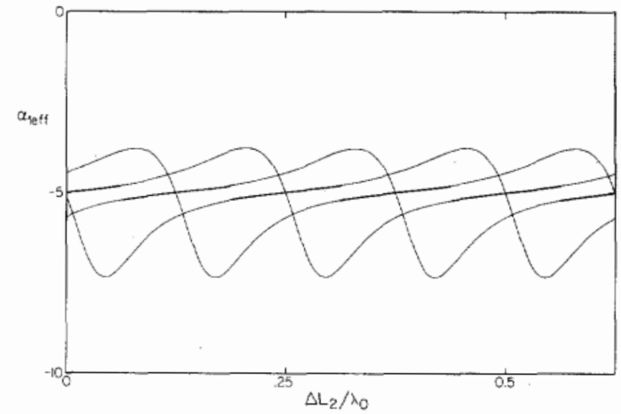

Fig. 5. Linewidth enhancement factor $\alpha_{1\text{eff}}$ versus cavity length for the device of Fig. 2.

ues of ν_i, we get a simultaneous increase in $g'_{1\text{eff}}$ (and related quantities, like the relaxation resonance frequency) and a decrease in $m'_{1\text{eff}}$ (and the phase modulation). In Figs. 4 ($K > 0$) and 12 ($K < 0$) we plot trajectories of $g'_{1\text{eff}}$ and $m'_{1\text{eff}}$ in the (g', m') plane which illustrate this mixing. The effective α-parameter, which determines the linewidth, can be written in terms of the coupling quantities and the material parameter α_1 as

$$\alpha_{1\text{eff}} \equiv \frac{m'_{1\text{eff}}}{g'_{1\text{eff}}} = \frac{\alpha_1(1+\nu_r) - \nu_i}{(1+\nu_r) + \alpha_1\nu_i}. \tag{63}$$

In Figs. 5 and 13 we plot $\alpha_{1\text{eff}}$ versus L_2 for the same set of parameters as in Figs. 2 and 10. It is clear that by varying the tuning of the laser $\alpha_{1\text{eff}}$ can be reduced, and since (with only one active element) (42) still applies, the linewidth may be reduced (or increased). A comparison of Figs. 5 and 13 shows that the potential for linewidth alteration is much greater for the $K > 0$ case than for $K < 0$; conveniently, that is also the case in which the gain selectivity between modes is highest (compare Figs. 2 and 10). If the coupling element between the active and passive cavity is lossless (e.g., a single mirror), then K is always negative. We see from Figs. 2 and 10, however, that the widest range of variation in $\alpha_{1\text{eff}}$ occurs for $K > 0$ (which occurs, for example, when the coupling is a gap of half-integral-wavelength spacing [11]). This result then suggests that by suitably coating the output facet of a passive–active resonator with a thick lossy coating, the linewidth could be reduced well below that which is otherwise attainable. It should be noted that such linewidth reduction predicted [25] and subsequently observed [26] by Vahala *et al.* and was explained in terms of a detuned loading mechanism, where the passive cavity became a frequency-dependent load upon the active one, and our $\nu_{r,i}$ plays the same role as the $\beta_{1,2}$ in their treatment. If the second cavity becomes active, however, then such a description is no longer applicable. The "load" becomes both frequency- and intensity-dependent, and it introduces noise of its own into the system. In the next section, we derive the relative intensity and frequency fluctuation spectra for a general two-active-element laser in terms of the effective modulation parameters, and explicitly evaluate them for a system consisting of two weakly coupled active cavities (e.g., a C^3 laser with a large air gap).

D. Active–Active Coupled Cavity

Let us first restrict ourselves to the case in which the fill factors Γ_i do not change appreciably under modulation, that is, we assume $c_{ij}\tau_i \ll 1$ for all ij pairs. This assumption will not qualitatively alter the physics, but it cuts down on the algebra considerably and renders the rather formidable expressions for the spectra somewhat more tractable. Then (31) and (32) give the responses to the Langevin sources

$$\tilde{\rho}(\Omega) = \frac{\tilde{\Delta} + \dfrac{g'_{1\text{eff}}}{j\Omega + 1/\tau_1}\tilde{\Xi}_1 + \dfrac{g'_{2\text{eff}}}{j\Omega + 1/\tau_2}\tilde{\Xi}_2}{j\Omega + \dfrac{\omega^2_{1\text{eff}}}{j\Omega + 1/\tau_1} + \dfrac{\omega^2_{2\text{eff}}}{j\Omega + 1/\tau_2}} \tag{64}$$

$$\begin{aligned}\Delta\tilde{\omega}(\Omega) = {}& \tilde{\Phi} + \tilde{\Delta}\,\frac{\alpha_{1\text{eff}}\dfrac{\omega^2_{1\text{eff}}}{j\Omega + 1/\tau_1} + \alpha_{2\text{eff}}\dfrac{\omega^2_{2\text{eff}}}{j\Omega + 1/\tau_2}}{j\Omega + \dfrac{\omega^2_{1\text{eff}}}{j\Omega + 1/\tau_1} + \dfrac{\omega^2_{2\text{eff}}}{j\Omega + 1/\tau_2}} \\ & - \tilde{\Xi}_1\,\frac{\dfrac{g'_{1\text{eff}}}{j\Omega + 1/\tau_1}\left[j\Omega\alpha_{1\text{eff}} + \dfrac{(\alpha_{1\text{eff}} - \alpha_{2\text{eff}})\,\omega^2_{2\text{eff}}}{j\Omega + 1/\rho_2}\right]}{j\Omega + \dfrac{\omega^2_{1\text{eff}}}{j\Omega + 1/\tau_1} + \dfrac{\omega^2_{2\text{eff}}}{j\Omega + 1/\tau_2}} \\ & - \tilde{\Xi}_2\,\frac{\dfrac{g'_{2\text{eff}}}{j\Omega + 1/\tau_2}\left[j\Omega\alpha_{2\text{eff}} + \dfrac{(\alpha_{2\text{eff}} - \alpha_{1\text{eff}})\,\omega^2_{1\text{eff}}}{j\Omega + 1/\tau_1}\right]}{j\Omega + \dfrac{\omega^2_{1\text{eff}}}{j\Omega + 1/\tau_1} + \dfrac{\omega^2_{2\text{eff}}}{j\Omega + 1/\tau_2}}.\end{aligned} \tag{65}$$

The relative intensity and field fluctuation spectra are then

$$W_{\rho\rho}(\Omega) = \frac{W_{\Delta\Delta} + \dfrac{g'^2_{1\text{eff}}W_{\Xi_1\Xi_1} + (2/\tau_1)\,g'_{1\text{eff}}W_{\Delta\Xi_1}}{\Omega^2 + 1/\tau_1^2} + \dfrac{g'^2_{2\text{eff}}W_{\Xi_2\Xi_2} + (2/\tau_2)\,g'_{2\text{eff}}W_{\Delta\Xi_2}}{\Omega^2 + 1/\tau_2^2}}{\left|j\Omega + \dfrac{\omega^2_{1\text{eff}}}{j\Omega + 1/\tau_1} + \dfrac{\omega^2_{2\text{eff}}}{j\Omega + 1/\tau_2}\right|^2} \tag{66}$$

$$W_{\omega\omega}(\Omega) = W_{\Phi\Phi} + W_{\Delta\Delta}\left|\frac{\alpha_{1\text{eff}}\dfrac{\omega_{1\text{eff}}^2}{j\Omega + 1/\tau_1} + \alpha_{2\text{eff}}\dfrac{\omega_{2\text{eff}}^2}{j\Omega + 1/\tau_2}}{j\Omega + \dfrac{\omega_{1\text{eff}}^2}{j\Omega + 1/\tau_1} + \dfrac{\omega_{2\text{eff}}^2}{j\Omega + 1/\tau_2}}\right|^2 + W_{\Xi_1\Xi_1}\left|\frac{g'_{1\text{eff}}\left[j\Omega\alpha_{1\text{eff}} + \dfrac{(\alpha_{1\text{eff}} - \alpha_{2\text{eff}})\,\omega_{2\text{eff}}^2}{j\Omega + 1/\tau_2}\right]}{j\Omega + 1/\tau_1 j\Omega + \dfrac{\omega_{1\text{eff}}^2}{j\Omega + 1/\tau_1} + \dfrac{\omega_{2\text{eff}}^2}{j\Omega + 1/\tau_2}}\right|^2$$

$$+ W_{\Xi_2\Xi_2}\left|\frac{g'_{2\text{eff}}\left[j\Omega\alpha_{2\text{eff}} + \dfrac{(\alpha_{2\text{eff}} - \alpha_{1\text{eff}})\,\omega_{1\text{eff}}^2}{j\Omega + 1/\tau_1}\right]}{j\Omega + 1/\tau_2 j\Omega + \dfrac{\omega_{1\text{eff}}^2}{j\Omega + 1/\tau_1} + \dfrac{\omega_{2\text{eff}}^2}{j\Omega + 1/\tau_2}}\right|^2$$

$$+ 2W_{\Delta\Xi_1}\frac{\text{Re}\left(\alpha_{1\text{eff}}\dfrac{\omega_{1\text{eff}}^2}{j\Omega + 1/\tau_1} + \alpha_{2\text{eff}}\dfrac{\omega_{2\text{eff}}^2}{j\Omega + 1/\tau_2}\right)\left(\dfrac{g'_{1\text{eff}}}{j\Omega + 1/\tau_1}\left[j\Omega\alpha_{1\text{eff}} + \dfrac{(\alpha_{1\text{eff}} - \alpha_{2\text{eff}})\,\omega_{2\text{eff}}^2}{j\Omega + 1/\tau_2}\right]\right)}{\left|j\Omega + \dfrac{\omega_{1\text{eff}}^2}{j\Omega + 1/\tau_1} + \dfrac{\omega_{2\text{eff}}^2}{j\Omega + 1/\tau_2}\right|^2}$$

$$+ 2W_{\Delta\Xi_2}\frac{\text{Re}\left(\alpha_{2\text{eff}}\dfrac{\omega_{2\text{eff}}^2}{j\Omega + 1/\tau_2} + \alpha_{1\text{eff}}\dfrac{\omega_{1\text{eff}}^2}{j\Omega + 1/\tau_1}\right)\left(\dfrac{g'_{2\text{eff}}}{j\Omega + 1/\tau_2}\left[j\Omega\alpha_{1\text{eff}} + \dfrac{(\alpha_{2\text{eff}} - \alpha_{1\text{eff}})\,\omega_{1\text{eff}}^2}{j\Omega + 1/\tau_1}\right]\right)}{\left|j\Omega + \dfrac{\omega_{1\text{eff}}^2}{j\Omega + 1/\tau_1} + \dfrac{\omega_{2\text{eff}}^2}{j\Omega + 1/\tau_2}\right|^2}. \quad (67)$$

A fundamental quantity of interest is the $\Omega = 0$ component of $W_{\omega\omega}$, since it gives the major contribution to the linewidth. We define for convenience the dimensionless ratios

$$x_1 \equiv \frac{\omega_{1\text{eff}}^2\tau_1}{\omega_{1\text{eff}}^2\tau_1 + \omega_{2\text{eff}}^2\tau_2}, \quad x_2 \equiv \frac{\omega_{2\text{eff}}^2\tau_2}{\omega_{1\text{eff}}^2\tau_1 + \omega_{2\text{eff}}^2\tau_2} \quad (68)$$

and produce from (67)

$$\begin{aligned} W_{\omega\omega}(\Omega = 0) = {} & W_{\Phi\Phi} + W_{\Delta\Delta}(\alpha_{1\text{eff}}x_1 + \alpha_{2\text{eff}}x_2)^2 \\ & + W_{\Xi_1\Xi_1}[g'_{1\text{eff}}\tau_1(\alpha_{1\text{eff}} - \alpha_{2\text{eff}})\,x_2]^2 \\ & + W_{\Xi_2\Xi_2}[g'_{2\text{eff}}\tau_2(\alpha_{2\text{eff}} - \alpha_{1\text{eff}})\,x_1]^2 \\ & + 2W_{\Delta\Xi_1}(\alpha_{1\text{eff}}x_1 + \alpha_{2\text{eff}}x_2) \\ & \cdot [g'_{1\text{eff}}\tau_1(\alpha_{1\text{eff}} - \alpha_{2\text{eff}})\,x_2] \\ & + 2W_{\Delta\Xi_2}(\alpha_{2\text{eff}}x_2 + \alpha_{1\text{eff}}x_1) \\ & \cdot [g'_{2\text{eff}}\tau_2(\alpha_{2\text{eff}} - \alpha_{1\text{eff}})\,x_1]. \end{aligned} \quad (69)$$

If we also make the assumption that $1/\tau_s << 1/\tau_{1,2}$; that is, that we are well above threshold, then these relations simplify when we insert the normalizations for the Langevin spectra. The cross-correlation terms $W_{\Delta\Xi_1}$ and $W_{\Delta\Xi_2}$ cancel each other out, and we are left with

$$\begin{aligned} W_{\omega\omega}(0) = {} & \frac{\eta_1 g_1\Gamma_1 V_1 + \eta_2 g_2\Gamma_2 V_2}{2pV^2} \\ & \cdot [1 + (\alpha_{1\text{eff}}x_1 + \alpha_{2\text{eff}}x_2)^2] \\ & + \frac{\eta_1 g_1\Gamma_1 V_2 + \eta_2 g_2\Gamma_2 V_1}{p\Gamma_1\Gamma_2 V_1 V_2} \\ & \cdot 2x_1x_2\left[\frac{g'_{1\text{eff}}}{g'_1}\right]\left[\frac{g'_{2\text{eff}}}{g'_2}\right](\alpha_{1\text{eff}} - \alpha_{2\text{eff}})^2 \end{aligned} \quad (70)$$

as the linewidth of a two-active element laser. The first part arises from optical fluctuations; in fact, it looks exactly like the enhanced Schawlow–Townes formula

$$W_{\omega\omega}(0) = \frac{\eta g}{2pV}(1 + \alpha^2) \quad (71)$$

where the material parameter α has been replaced by a weighted average of the effective $\alpha_{i\text{eff}}$'s. The second part arises from the $W_{\Xi\Xi}$'s, and represents direct FM due to carrier fluctuations. It is proportional to the square of the difference in the effective α's. Consequently, were we to attempt to utilize detuned loading to change the effective α's and shrink the linewidth, we should not only seek to reduce the effective α's, but at the same time to minimize their difference. Both contributions to the linewidth vary with inverse power. Equation (70) holds for any two-active-element laser C^3, axially groove-coupled, or laterally coupled cavity. The evaluation of $\alpha_{1\text{eff}}$ and $\alpha_{2\text{eff}}$ depends on the exact configuration, however, so we will now evaluate them for the case of two weakly coupled active cavities. We can adapt some of our results from the passive–active case by making cavity (2) of Fig. 1 an active one, with gain γ_2 and index μ_2 both dependent upon the carrier density n_2 in cavity 2. Equations (49) and (50) remain valid if we redefine

$$\begin{aligned} \varphi_1(\omega) &\equiv -(\gamma_1 - \gamma_0)\,L_1 + 2j\omega\mu_1 L_1/c - \ln R_1R_2, \\ \varphi_2(\omega) &\equiv -(\gamma_2 - \gamma_0)\,L_2 + 2j\omega\mu_2 L_2/c - \ln R_3R_2. \end{aligned} \quad (72)$$

As with the passive–active case, the resonance equation is transcendental. For weak coupling, we can again perform a perturbation series in K, although it is not clear whether our zeroth-order equation should be

$$[e^{\varphi_1(\omega_0)} - 1] = 0 \quad \text{or} \quad [e^{\varphi_2(\omega_0)} - 1] = 0. \tag{73}$$

For weak coupling, there will be two families of modes, one associated with each of the two equations in (73). So, we will consider only the modes in which cavity 1 is dominant, and cavity 2 assumes the role of the frequency-dependent loss. There is still one degree of freedom left unaccounted for (in a two-element laser, the gain is clamped onto a line in the (γ_1, γ_2)-plane, rather than a point [20]) so we will take γ_2 as the free parameter. If we use the following as the definition of $\varphi_2(\omega_0)$,

$$\begin{aligned}\varphi_2(\omega_0) = 2j \frac{\mu_2 L_2}{\mu_1 L_1} k\pi - (\gamma_2 - \gamma_0) L_2 \\ + \frac{\mu_2 L_2}{\mu_1 L_1} (\gamma_1 - \gamma_0) L_1 \\ + \frac{\mu_2 L_2}{\mu_1 L_1} \ln R_1 R_2 - \ln R_2 R_3\end{aligned} \tag{74}$$

then (53), (54) and (56)–(59) give the correct results for $\overline{\omega}$, $\gamma_1(n_{1\text{th}})$, $g'_{1\text{eff}}$ and $m'_{1\text{eff}}$. Differentiating (56) with respect to n_2 yields

$$\begin{aligned}\begin{Bmatrix} g'_{2\text{eff}} \\ m'_{2\text{eff}} \end{Bmatrix} = \begin{Bmatrix} \text{Im} \\ \text{Re} \end{Bmatrix} \left(\frac{\overline{\omega}\mu'_2}{\mu_2} - \frac{1}{2j} \frac{\gamma'_2 c}{2\mu_2} \right) \\ \cdot \left(K \frac{\mu_2 L_2}{\mu_1 L_1} \frac{e^{\varphi_2(\omega_0)}}{[e^{\varphi_2(\omega_0)} - 1]^2} \right)\end{aligned} \tag{75}$$

or, recognizing ν of (61) (using the appropriate $\varphi_2(\omega_0)$, of course) and the material quantities

$$g'_2 = \frac{\gamma'_2 c}{2\mu_2}, \quad m'_2 \equiv \frac{\overline{\omega}\mu'_2}{\mu_2}.$$

The effective differential quantities are given by

$$g'_{2\text{eff}} = g'_2 \nu_r + m'_2 \nu_i, \quad m'_{2\text{eff}} = m'_2 \nu_r - g'_2 \nu_i. \tag{76}$$

Consequently, the effective linewidth enhancement factors that enter into equation (71) are given by

$$\alpha_{1\text{eff}} = \frac{\alpha_1(1 + \nu_r) - \nu_i}{(1 + \nu_r) + \alpha_1 \nu_i}, \quad \alpha_{2\text{eff}} = \frac{\alpha_2 \nu_r - \nu_i}{\nu_r + \alpha_2 \nu_i}. \tag{77}$$

In a two-active-element laser both L_1 and L_2 are fixed and what varies the tuning is the gain and index γ_2 and μ_2, so in Figs. 6–9 and 14–17 we plot the gain, lasing frequency, effective α's and linewidth versus γ_2 for $K = \pm 0.4$. A cursory inspection of Fig. 8(b) and (76) shows that it is quite possible for $g'_{2\text{eff}}$ to go to zero, in which case $\alpha_{2\text{eff}} \to \infty$, and the linewidth would seem to diverge as well. However, there are $g'_{2\text{eff}}$-dependent terms in (70) (e.g., x_2) which remove the apparent singularity. In this case, the direct FM contribution to linewidth can be written as

$$W^{\text{FM}}_{\omega\omega}(0) = \frac{2}{p} \left(\frac{\eta_1 g_1}{\Gamma_2 V_2} + \frac{\eta_2 g_2}{\Gamma_1 V_1} \right) \left(\frac{g_2}{g_1} \right) \left(\frac{m'_{2\text{eff}}}{m'_2} \right)^2 \alpha_2^2 \tag{78}$$

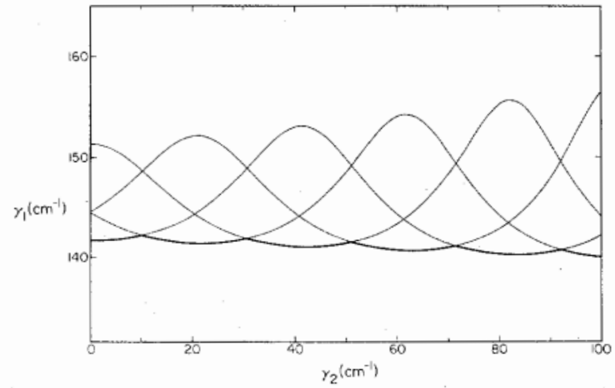

Fig. 6. Threshold gain for several modes of a (200–50 μm) active–active laser versus gain γ_2 in cavity 2, with a coupling factor $K = -0.4$.

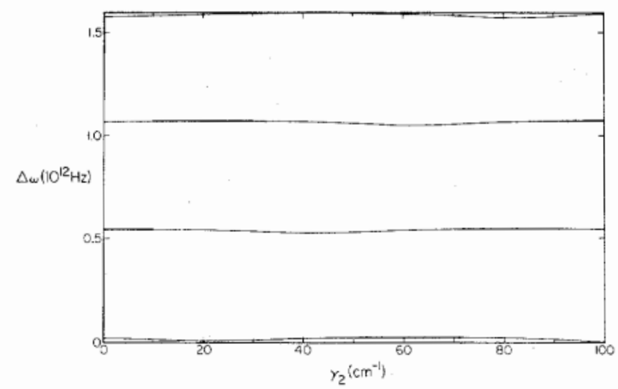

Fig. 7. Lasing frequency versus γ_2 for the device of Fig. 6.

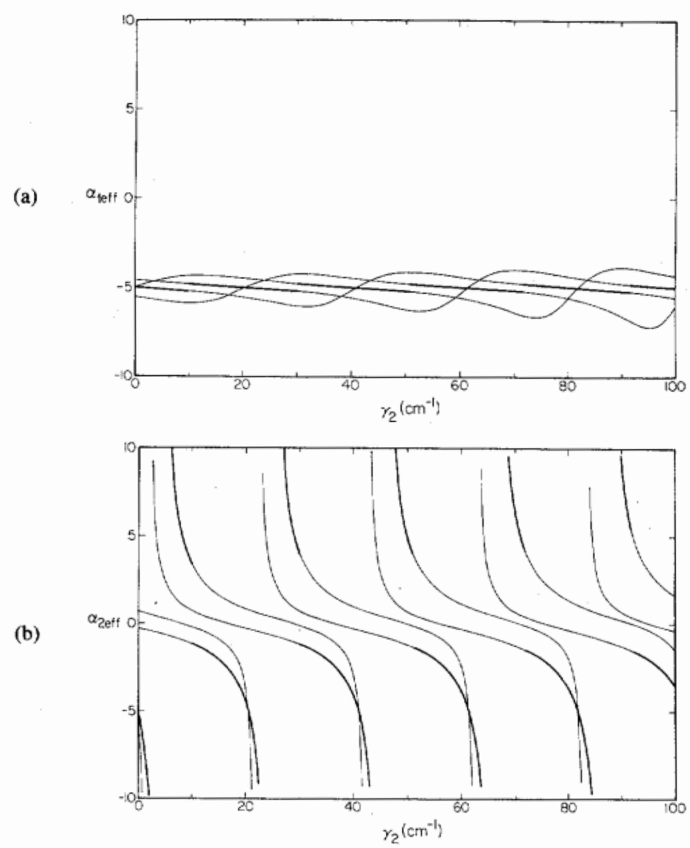

Fig. 8. Effective α-parameters for the device of Fig. 6. (a) $\alpha_{1\text{eff}}$, (b) $\alpha_{2\text{eff}}$.

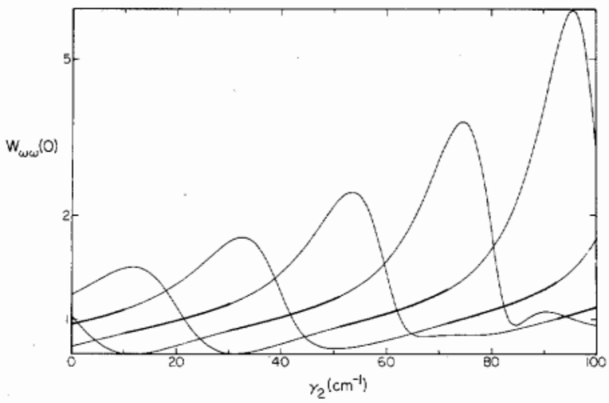

Fig. 9. Linewidth of the device of Fig. 6 as a function of γ_2 (logarithmic scale) relative to that of a single-element cavity of length 250:mm, reflectivities R_1, R_3 at the end mirrors.

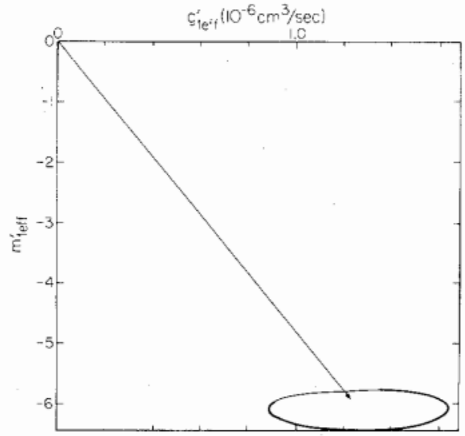

Fig. 12. Trajectory of $g'_{1\text{eff}}$, $m'_{1\text{eff}}$ for the device of Fig. 10.

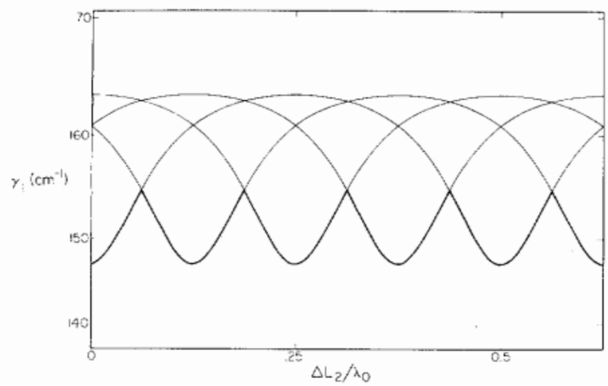

Fig. 10. Threshold gain for several modes of a passive–active laser with coupling factor $K = +0.4$.

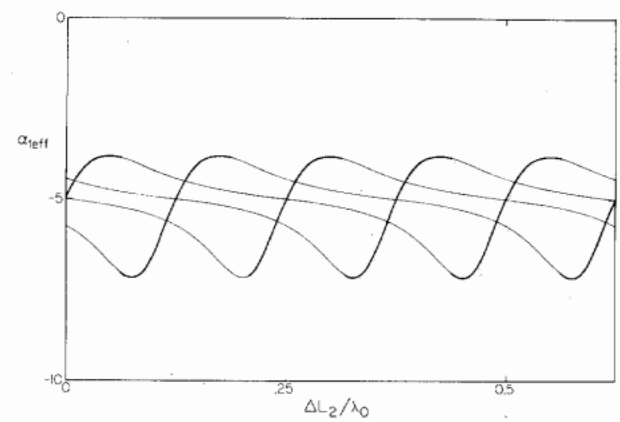

Fig. 13. Linewidth enhancement factor $\alpha_{1\text{eff}}$ for the device of Fig. 10.

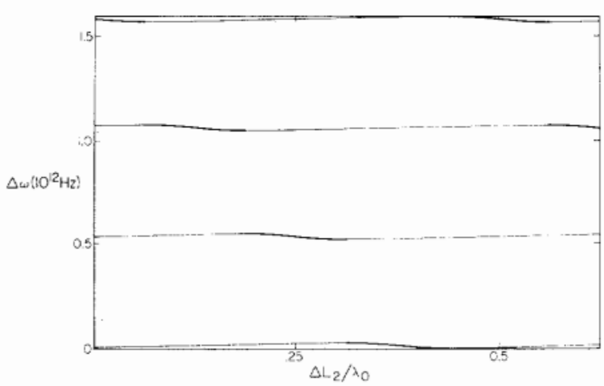

Fig. 11. Lasing frequency versus cavity length for the device of Fig. 10.

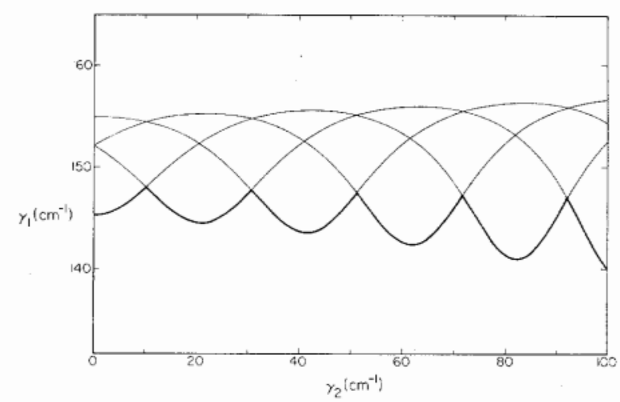

Fig. 14. Threshold gain for an active–active cavity versus γ_2 for a coupling factor $K = +0.4$.

where α_2 is the material α for cavity 2. The chirp (direct FM under modulation) in an active–active coupled-cavity laser has been shown to be proportional to the difference in effective α's [15]; in (70), we showed that there is a component of the linewidth which scales with this difference. Consequently, it would be desirable to reduce both the chirp and linewidth by tuning the α's to be equal. Assuming that the material α's are equal (and denoting them by α devoid of subscript), the difference in the effective α's is given by

$$(\alpha_{1\text{eff}} - \alpha_{2\text{eff}}) = \frac{\alpha(1 + \nu_r) - \upsilon_i}{(1 + \nu_r) + \alpha\nu_i} - \frac{\alpha\nu_r - \nu_i}{\nu_r + \alpha\nu_i}$$
$$= \frac{\nu_i(1 + \alpha^2)}{[(1 + \nu_r) + \alpha\nu_i][\nu_r + \alpha\nu_i]}. \quad (79)$$

So when $\nu_i = 0$, the cavity is tuned at the chirpless bias point. At that point, however, we see from (77) that $\alpha_{1\text{eff}} = \alpha_{2\text{eff}} = \alpha$, the material linewidth enhancement factor. The upshot of this result is that while we can eliminate

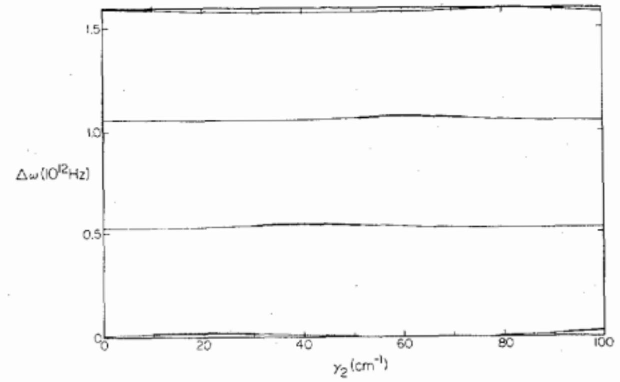

Fig. 15. Lasing frequency versus γ_2 for device of Fig. 14.

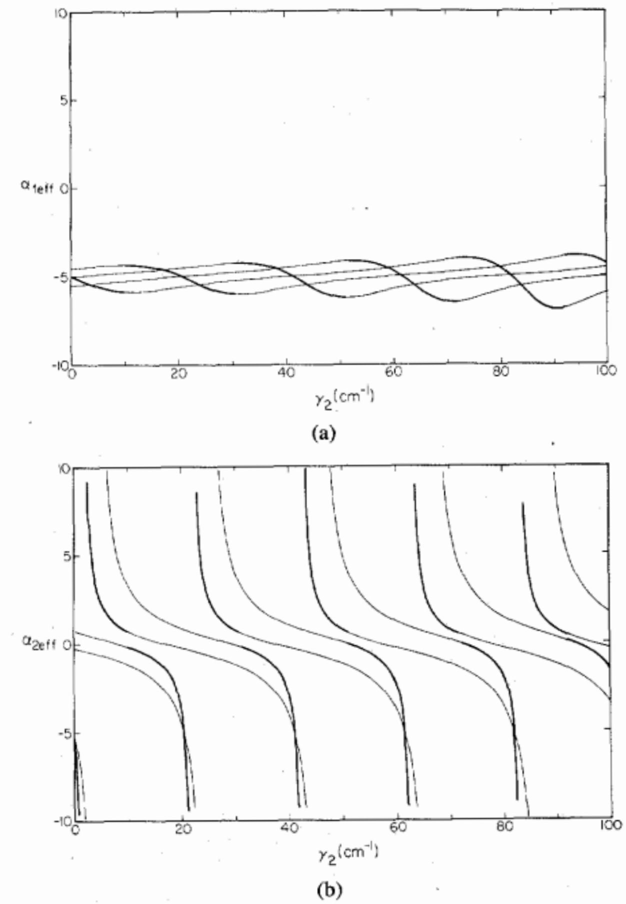

Fig. 16. Effective α-parameters for device of Fig. 14. (a) $\alpha_{1\text{eff}}$, (b) $\alpha_{2\text{eff}}$.

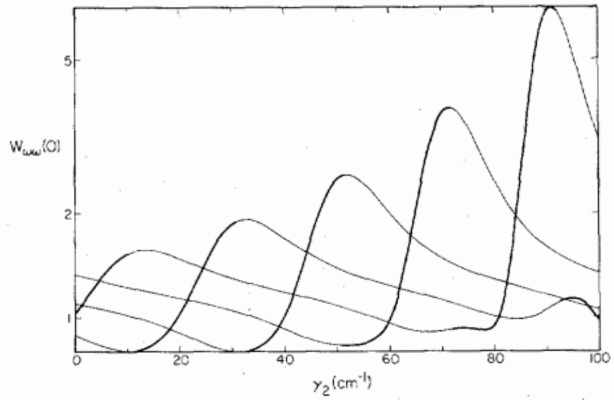

Fig. 17. Linewidth of the device of Fig. 14 relative to that of an equivalent single-element laser (logarithmic scale).

chirp in two-active element lasers by selection of bias point, we give up the potential for linewidth reduction using the detuned loading mechanism that was possible with the passive–active cavity. Conversely, any attempt to reduce the linewidth through detuned loading will result in a chirp under modulation. Another feature is that the largest linewidth excursions occur near a mode hop, so that the mode selectivity is likely to be low when tuned to a narrow linewidth. On the other hand, one could locate the narrow-linewidth regions by tuning to the vicinity of a mode hop. Although it has been shown that away from the zero-chirp bias point, the chirp may be reduced by driving both of the cavities with a fixed amplitude relationship [13], this modulation will not affect the noise properties. Consequently, the linewidth of the laser may still be larger than that at the zero-chirp point due to the FM contribution. It must be noted that (76)–(79) are based on the assumption of weakly-coupled cavities; for two strongly coupled cavities, one must numerically solve the transcendental dispersion equation for the threshold gain and lasing frequency (although once in possession of those quantities, (8) may be evaluated directly for the effective modulation parameters). We expect, however, that the results of the perturbation analysis will still hold qualitatively. With strong coupling, the modulation quantities should vary even more widely from their material values, yielding larger excursions of the linewidth and other functions of noise (as well as dynamic quantities, like the relaxation resonance). The formalism presented in this section is easily applicable to larger ensembles of coupled cavities since the matrices in (30)–(33) are general and the dispersion function $F(\omega, n_1, \cdots, n_n)$ is usually straightforward to derive. However, the complexity and large number of degrees of freedom in such a device will likely limit its technological significance.

V. Conclusions

In summary, we have provided a formalism for calculating any spectral function of an arbitrary multielement semiconductor laser. We carried out the analysis for a single-active element laser and showed that the spectra obtained were identical to those calculated from the more conventional theory. When a passive element is added to the system, the material differential gain and index constants are replaced by effective quantities which can be calculated from the dispersion equation. For the case of a passive resonator weakly coupled to an active one, we found approximate solutions for the lasing frequency, threshold, and effective modulation quantities consistent with prior results. The effective parameters were shown to be mixtures of the material parameters, with the relative contributions determined by the relative tuning of the two cavities.

We then calculated expressions for the relative intensity and frequency fluctuation spectra of a device with two active elements, e.g., a C^3 laser. We derived formulas which defined the effective modulation parameters, and for the special case of a subthreshold cavity ("modulator") weakly coupled to another active cavity we produced approximate solutions for the gain and lasing frequency as a function of carrier density in the modulator cavity. We also gave simple expressions for the effective modulation quantities in terms of the material parameters and a single complex constant which determines the amount of mixing. For the weakly coupled geometry, the cavities can be adjusted so that there is no chirp under modulation, but in that case, it is not possible to reduce the linewidth below the enhanced Schawlow-Townes limit with detuned loading. On the other hand, if the laser is not biased to the zero-chirp condition, the linewidth may be increased or decreased beyond that given by the enhanced Schawlow-Townes formula, depending upon the tuning of the cavity.

Acknowledgment

The authors would like to acknowledge fruitful discussions with Dr. K. Vahala.

References

[1] M. Nakamura, K. Aiki, J.-I. Umeda, A. Yariv, H. W. Yen, and T. Morkawa, "GaAs-GaAlAs double heterostructure distributed feedback diode lasers," *Appl. Phys. Lett.*, vol. 25, pp. 487-488, 1974.

[2] H. W. Yen, W. Ng, I. Samid, and A. Yariv, "GaAs distributed Bragg reflector lasers," *Opt. Commun.*, vol. 17, pp. 213-218, 1976.

[3] W. T. Tsang and N. A. Olsson, "High speed direct single-frequency modulation with large tuning rate and frequency excursion in cleaved-coupled-cavity semiconductor lasers," *Appl. Phys. Lett.*, vol. 42, pp. 650-652, 1983.

[4] K. J. Ebeling, L. A. Coldren, B. I. Miller, and J. A. Rentschler, "Single-mode operation of coupled-cavity GaInAsP/InP semiconductor lasers," *Appl. Phys. Lett.*, vol. 42, pp. 6-8, 1983.

[5] J. Salzman, R. Lang, and A. Yariv, "The laterally coupled cavity laser," *Appl. Phys. Lett.*, vol. 47, pp. 195-197, 1985.

[6] J. Katz, E. Kapon, C. Lindsey, S. Margalit, U. Shreter, and A. Yariv, "Phased-locked semiconductor laser array with separate contacts," *Appl. Phys. Lett.*, vol. 43, pp. 521-523, 1983.

[7] D. Marcuse and T.-P. Lee, "Rate equation model of a coupled-cavity laser," *IEEE J. Quantum Electron.*, vol. QE-20, pp. 166-176, 1984.

[8] H. K. Choi, K.-L. Chen, and S. Wang, "Analysis of two-section coupled-cavity semiconductor lasers," *IEEE J. Quantum Electron.*, vol. QE-20, pp. 385-393, 1984.

[9] L. Coldren and T. L. Koch, "Analysis and design of coupled-cavity lasers—Part I: Threshold gain analysis and design guidelines," *IEEE J. Quantum Electron.*, vol. QE-20, pp. 659-682, 1984.

[10] W. Streifer, D. Yevick, T. L. Paoli, and R. D. Burnham, "An analysis of cleaved coupled-cavity lasers," *IEEE J. Quantum Electron.*, vol. QE-20, pp. 754-764, 1984.

[11] C. H. Henry and R. F. Kazarinov, "Stabilization of single-frequency operation of coupled-cavity lasers," *IEEE J. Quantum Electron.*, vol. QE-20, pp. 733-744, 1984.

[12] G. Agrawal, "Coupled-cavity semiconductor lasers under current modulation: Small-signal analysis," *IEEE J. Quantum Electron.*, vol. QE-21, pp. 255-263, 1985.

[13] L. A. Coldren, G. D. Boyd, J. E. Bowers, and C. A. Burrus, "Reduced dynamic linewidth in three-terminal two-section diode lasers," *Appl. Phys. Lett.*, vol. 46, pp. 125-127, 1985.

[14] W. Streifer, D. Yevick, T. L. Paoli, and R. D. Burnham, "Cleaved-coupled cavity laser analysis," presented at the OSA, San Diego, CA, Oct. 29-Nov. 2, 1984.

[15] R. Lang and A. Yariv, "Dynamic analysis of multielement semiconductor lasers," *IEEE J. Quantum Electron.*, vol. QE-21, pp. 1683-1688, 1985.

[16] T. L. Paoli and J. E. Ripper, "Observations of intrinsic quantum fluctuations in semiconductor lasers," *Phys. Rev.*, vol. 2, pp. 2551-2555, 1970.

[17] D. E. McCumber, "Intensity fluctuations in the output of CW laser oscillators I," *Phys. Rev.*, vol. 141, pp. 306-322, 1966.

[18] K. Vahala, Ch. Harder, and A. Yariv, "Observations of relaxation resonance effects in the field spectrum of semiconductor lasers," *Appl. Phys. Lett.*, vol. 42, pp. 211-213, 1983.

[19] M. Fleming and A. Mooradian, "Fundamental line broadening of single mode (GaAl)As diode lasers," *Appl. Phys. Lett.*, pp. 511-513, 1981.

[20] C. H. Henry, "Theory of the linewidth of semiconductor lasers," *IEEE J. Quantum Electron.*, vol. QE-18, pp. 259-264, 1982.

[21] D. Welford and A. Mooradian, "Observations of linewidth broadening in (GaAl)As diode lasers due to electron number fluctuations," *Appl. Phys. Lett.*, vol. 40, pp. 560-562, 1982.

[22] G. Tenchio, "Low frequency intensity fluctuations of CW DH GaAlAs diode lasers," *Electron. Lett.*, vol. 12, p. 562, 1976.

[23] G. Tenchio, "1/f noise of continuous-wave semiconductor lasers," *Electron. Lett.*, vol. 13, p. 614, 1977.

[24] A. Dandridge and A. B. Tveten, "Phase noise of single-mode diode lasers in interferometer systems," *Appl. Phys. Lett.*, vol. 39, pp. 530-532, 1981.

[25] K. Vahala and A. Yariv, "Detuned loading in coupled cavity semiconductor lasers—Effect on quantum noise and dynamics," *Appl. Phys. Lett.*, vol. 45, pp. 501-503, 1984.

[26] K. Vahala, J. Paslaski, and A. Yariv, "Observation of modulation speed enhancement, frequency modulation suppression and phase noise reduction by detuned loading in a coupled-cavity semiconductor laser," *Appl. Phys. Lett.*, vol. 46, pp. 1025-1027, 1985.

[27] K. Vahala and A. Yariv, "Semiclassical theory of noise in semiconductor lasers—Part II," *IEEE J. Quantum Electron.*, vol. QE-19, pp. 1102-1109, 1983.

[28] R. Lang, K. Vahala, and A. Yariv, "The effect of spatially dependent temperature and carrier fluctuations on noise in semiconductor lasers," *IEEE J. Quantum Electron.*, vol. QE-21, pp. 443-451, 1985.

[29] M. Lax, "Quantum noise IX: Quantum theory of noise sources," *Phys. Rev.*, vol. 145, pp. 110-121, 1965.

[30] H. Haug and H. Haken, "Theory of noise in semiconductor laser emission," *Z. Phys.*, vol. 204, pp. 262-275, 1967.

Robert J. Lang (S'83) was born in Dayton, OH, on May 4, 1961, and was raised in Atlanta, GA. In 1982 he received the B.S. degree in electrical engineering from the California Institute of Technology, Pasadena, CA. He received the M.S. degree, also in electrical engineering, from Stanford University, Stanford, CA.

Currently, he has been pursuing the Ph.D. degree in applied physics at the California Institute of Technology, where he is investigating dynamic and spectral properties of semiconductor lasers. He has written numerous articles and two books.

Amnon Yariv (S'56-M'59-F'70) was born in Tel Aviv, Israel, on April 13, 1930. He received the B.S., M.S., and Ph.D. degrees in electrical engineering from the University of California, Berkeley, in 1954, 1956, and 1958, respectively.

A veteran of the Israeli war of independence, he came to the United States in 1951. He went to Bell Laboratories, Murray Hill, NJ, in 1959, joining the early stages of the laser effort. He joined the California Institute of Technology, Pasadena, in 1964, as an Associate Professor of Electrical Engineering, becoming a Professor in 1966. In 1980 he became the Thomas G. Myers Professor of Electrical Engineering and Applied Physics. On the technical side, he took part (with various co-workers) in the discovery of a number of early solid-state laser systems, in the formulation of the theory

of parametric quantum noise and the prediction of parametric fluorescence, in the invention of the technique of mode-locked ultrashort-pulse lasers and FM lasers, in the introduction of GaAs and CdTe as infrared electrooptic and window materials, in proposing and demonstrating semiconductor-based integrated optics technology, and in pioneering the field of phase conjugate optics. His present research efforts are in the areas of nonlinear optics, recombination mechanisms in semiconductors, semiconductor lasers and integrated optics, especially the problem of monolithic integration of transistors, injection lasers, and detectors for high-frequency applications. He authored or coauthored some 300 papers in professional journals, as well as a number of basic texts in quantum electronics, optics, and quantum mechanics. He is a Consultant to the Hughes Aircraft Research Laboratories, and is a founder and Chairman of the Board of Ortel Corporation, Alhambra, CA.

Dr. Yariv is a member of the American Physical Society, Phi Beta Kappa, and the National Academy of Engineering, and a Fellow of the Optical Society of America. He was the recipient of the 1980 Quantum Electronics Award of the IEEE. He is also an Associate Editor of *Optics Communications* and the *Journal of Applied Physics*, and was previously Associate Editor of the IEEE JOURNAL OF QUANTUM ELECTRONICS.